Hindawi
Journal of Chemistry
Volume 2020, Article ID 7459042, 9 pages
https://doi.org/10.1155/2020/7459042

Research Article

Synthesis of Zinc Oxide Nanoparticles Using Leaf Extract of *Lippia adoensis* (Koseret) and Evaluation of Its Antibacterial Activity

Meron Girma Demissie, Fedlu Kedir Sabir, Gemechu Deressa Edossa, and Bedasa Abdisa Gonfa

Adama Science and Technology University, School of Applied Natural Science, Departments of Applied Chemistry, P.O. Box 1888, Adama, Ethiopia

Correspondence should be addressed to Bedasa Abdisa Gonfa; bedassa.abdissa@astu.edu.et

Received 28 April 2020; Revised 6 August 2020; Accepted 24 September 2020; Published 20 October 2020

Academic Editor: Barbara Gawdzik

The synthesis of metal oxide nanoparticles with the use of medicinal plant extract is a promising alternative to the conventional chemical method. This work aimed to synthesize zinc oxide nanoparticles using a green approach from indigenous "Koseret" *Lippia adoensis* leaf extract which is an endemic medicinal plant and cultivated in home gardens of different regions of Ethiopia. The biosynthesized zinc oxide nanoparticles were characterized using thermogravimetric analysis, X-ray diffraction, scanning electron microscopy-energy dispersive spectroscopy, transmission electron microscopy, ultraviolet-visible spectroscopy, and Fourier transform infrared spectroscopy. Furthermore, this study also evaluated the antibacterial activity of the synthesized ZnO nanoparticles against clinical and standard strains of *Escherichia coli*, *Klebsiella pneumonia*, *Staphylococcus aureus*, and *Enterococcus faecalis* by the disc diffusion method. According to the result of this study, ZnO nanoparticles synthesized using *Lippia adoensis* leaf extract showed promising result against both Gram-positive and Gram-negative bacterial strains with a maximum inhibition zone of 14 mm and 12 mm, respectively, using uncalcinated form of the synthesized ZnO nanoparticles.

1. Introduction

The rise and development of nanotechnology has brought to the world a new potential and broader perspective of what humanity can achieve through material manipulation at the nanoscale and introduced a global paradigm shift in life because of its applications in various fields [1–5]. Compared to their mass complements, nanoparticles (NPs) demonstrate a peculiar nature of having a large surface to volume ratio that constructs themselves as more suitable candidates in application-oriented performances [6]. The novel properties of nanoparticles are widely deployed for various applications in medicine, cosmetics, biomedical devices, environmental remediation, electronics, photocatalysis, energy reservoirs, agriculture, automobiles, packaging, and information technology [7–13]. Among the available large number of nanoparticles, metal oxide nanoparticles are considered to be more promising as they exhibit unique physical, chemical, and biological properties [7]. In the synthesis process of nanoparticles, the use of toxic chemicals for the reduction and as a capping agent leads to various side effects and toxicity. As a result, the synthesis of metal oxide nanoparticles through plant extracts has gained importance. This approach is ecofriendly and has a higher reaction rate compared to conventional chemicals. Plant extracts contain various active biomolecules that help in the reduction and stability of nanoparticles [6, 12]. Zinc oxide (ZnO) is gaining attention by researchers in the recent past owing to its unique properties and abundant applications [14–17]. Based on the previous literature reports, ZnO nanoparticles have been synthesized from various plant extracts such as *Azadirachta indica* [18, 19], *Passiflora caerulea* [20], *Aloe vera* [13, 21], *Vitex trifolia* [22], *Trifolium pratense* [23], *Bauhinia tomentosa* [24], *Cinnamomum verum* [25], *Camellia sinensis* [26], *Artocarpus gomezianus* [27], *Duranta erecta* [28], *Moringa oleifera* [29], *Matricaria chamomilla*, *Olea*

europaea, and *Lycopersicon esculentum* [30], and their antimicrobial activities were also reported.

In the present study, *Lippia adoensis* leaf extracts were considered for the synthesis of nanoparticles as this is the first ever report on the plant being utilized for green synthesis of nanoparticles. *Lippia* species is an endemic medicinal plant to Ethiopia and cultivated in home gardens in different regions of Ethiopia with an altitudinal range of 1600–2200 m. The leaves of *Lippia adoensis* are used in Ethiopian traditional medicine for the treatment of various skin diseases including eczema and superficial fungal infections [31]. Furthermore, the antibacterial activity profile of *Lippia adoensis* against bacterial strains was investigated, and the result indicated that Gram-positive bacteria (*S. aureus)* were shown to be more susceptible than Gram-negative bacteria (*E. coli*, *Salmonella typhi*, and *P. aeruginosa*) [31, 32]. Therefore, this work aimed to explore the application of *Lippia adoensis* leaves extract as a capping and reducing agent for the synthesis of ZnO NPs in addition to its various traditional applications and evaluate the antibacterial activities of the synthesized ZnO NPs against pathogenic organisms using the agar disc diffusion method. Furthermore, this work opens up a door for further explorations on many of Ethiopians indigenous plants for nanomaterial synthesis which could be used for various applications.

2. Materials and Methods

2.1. Collection and Preparation of Plant Material (Broth Solution). Collected fresh leaves of *Lippia adoensis* "Koseret" were thoroughly washed using tap and distilled water to remove the dust particles and sun dried to remove the residual moisture. The dried leaves were ground into powder and sieved by using 150 μm size sieves. The aqueous extracts of the sample were prepared by boiling 5 g of fine powdered leaves in 100 ml of double distilled water at 80°C for 60 minutes while stirring using a magnetic stirrer at 800 rpm. The extract was then cooled to room temperature and filtered using Whatman No.1 filter paper and stored in a refrigerator at 4°C for further experimental use [33].

2.2. Biosynthesis of ZnO NPs. 1 : 1 (50 mL *Lippia adoensis* extract and 50 mL of 0.45 M zinc acetate dihydrate), 3 : 2 (60 mL *Lippia adoensis* extract and 40 mL of 0.45 M zinc acetate dihydrate), and 9 : 1 (90 mL *Lippia adoensis* extract and 10 mL of 0.45 M zinc acetate dihydrate) ratios were mixed with 50 mL, 40 mL, and 10 mL of 0.45 M NaOH, respectively. The three mixtures were then stirred continuously for 2 hrs using a magnetic stirrer at 800 rpm that resulted in yellow precipitate formation. The precipitates were then filtered using a glass filter and washed repeatedly with distilled water followed by ethanol in order to remove the impurities and oven dried at 100°C for 1 hr. The obtained dried light yellow color powders were mashed using a mortar and pestle. Finally, after conducting thermal stability of the biosynthesized nanoparticles, the mashed yellow powders were calcined at 400°C for 1 hr and fine ground and made ready for further characterizations [33].

2.3. Characterization of Biosynthesized ZnO NPs. Thermal gravimetric analysis was carried out using a simultaneous DTA-TGA (DTG-60H, Shimadzu Co., Japan) analysis to analyze the decomposition and thermal stability of the biosynthesized ZnO NPs measured at the heating rate of 10°C/min. Crystalline structure and the average crystalline size of the synthesized ZnO NPs were characterized using an X-ray diffractometer (XRD-7000, Shimadzu Co., Japan) equipped with a Cu target for generating a CuKα radiation with $\lambda = 1.54056$ Å. XRD spectra were recorded from 10° to 80° with 2θ angles using CuKα radiation operated at 40 kV and 30 mA. The crystallite sizes (D) of the powders were calculated by using Scherrer's equation:

$$D = \frac{0.94\lambda}{\beta \cos\theta}, \quad (1)$$

where $K = 0.94$ is Scherrer's constant, λ is the X-ray wavelength, θ is Bragg's diffraction angle, and β is the peak width of the diffraction line at half of the maximum intensity.

To analyze the morphology and composition, the biosynthesized ZnO NPs were characterized by field emission scanning electron microscopy equipped with energy dispersive X-ray spectroscopy (FE-SEM, JEOL-JSM 6500F, made in Japan). Furthermore, to analyze the shape, particle size, and crystallinity, the biosynthesized ZnO NPs were characterized using high-resolution transmission electron microscopy (HRTEM, Tecnai F20 G2, Philips, Netherlands) at an accelerating voltage of 200 kV. The absorption spectra of the biosynthesized ZnO NPs were recorded by using JASCO V-670 UV-Vis spectroscopy equipped with a diffuse reflectance attachment for powder samples in between a wavelength scan of 200 and 800 nm. The biosynthesized ZnO NPs were also characterized using Fourier transform infrared spectroscopy (FTIR, Perkin Elmer 65) to analyze and detect surface functional groups in the scanning range of 4000–400 cm^{-1}.

2.4. Antibacterial Activity Analysis of Biosynthesized ZnO NPs. The antibacterial activity of ZnO nanoparticles (calcined and uncalcined) on Gram-positive (*Staphylococcus aureus* and *Enterococcus faecalis*) and Gram-negative (*Escherichia coli* and *Klebsiella pneumonia*) bacteria was tested by the disc diffusion method according to the procedures reported [34]. Microbial strains were grown aerobically in nutrient broth for 24 hrs at 37°C until the turbidity of bacterial suspensions was achieved to 1.5×10^8 CFU/mL by comparison with the 0.5 McFarland standard. Bacterial cultures were maintained on nutrient Muller–Hinton agar at 37°C, the antibiotics vancomycin and carbenicillin were used as the positive control (PC), and dimethyl sulfoxide (DMSO) solvent was used as the negative control (NC).

The plates were then turned upside down and incubated at 37°C for 24 hrs in an incubator. The plates were shaken gently to allow equal mixing of bacteria cells and agar.

60 mm plate that accommodated two discs and ZnO nanoparticles without unacceptable overlapping of zones was used. Agar plate was divided into 3 sections: antibiotic disc, ZnO nanoparticle sample, and both antibiotic disc and ZnO nanoparticle sample. Then, 100 mg of ZnO nanoparticles were dissolved in 200 μL of DMSO. From the prepared sample, 200 μL of each concentration were diluted in 200 and 400 μL of DMSO solvent to obtain 1 : 4 and 1 : 8 dilution factors. From each sample, 200 μL of each concentration saturated with discs (6 mm diameter disc) was placed on a plate and incubated at 37°C for 24 hrs. Antibacterial activity was then evaluated by measuring the diameter (mm) of the inhibition zone (IZ) around the disc against the test organisms by using a caliper.

3. Results and Discussion

3.1. Thermogravimetric Analysis (TGA). Figure 1 shows the thermogravimetric analysis (TGA) and differential thermal analysis (DTA) of the uncalcined ZnO nanoparticles (9 : 1 UZnO). TGA curve shows mass loss of the sample, whereas the DTA curve indicates the energy gain or loss during the process. TGA/DTA transition shows a loss of 36.270% up to 400°C, and no considerable loss in mass is observed after this temperature up to 1000°C. This indicates that the biosynthesized ZnO nanoparticles are thermally stable after 400°C. Therefore, temperature of 400°C was used as calcination temperature for all other synthesized ZnO nanoparticles during this work.

3.2. X-Ray Diffraction (XRD) Analysis. Figure 2 shows the XRD pattern of ZnO nanoparticles synthesized using zinc acetate dihydrate and *Lippia adoensis* leaf extract using five different ratios by volume. The formation of biosynthesized ZnO NPs was also confirmed by X-ray diffraction measurements. The diffraction peaks appeared at a 2θ value of ≈31.76°, 34.42°, 36.24°, 47.54°, 56.59°, 62.86°, 66.41°, 67.97°, and 69.06° corresponding to (100), (002), (101), (102), (110), (103), (200), (112), and (201) crystal planes, respectively, which is in agreement with the previously reported work [34]. All the diffraction peaks were properly assigned using the JCPDS file card No. 0361451, and characteristic peaks for pure ZnO were observed in the XRD patterns confirming the formation of ZnO NPs synthesized by using *Lippia adoensis* leaf extract and zinc acetate dihydrate. Furthermore, XRD analysis also showed that all the diffraction peaks fit well with the hexagonal wurtzite structure of ZnO NPs [23, 35]. The average crystal size of the biosynthesized ZnO nanoparticles was determined from the three most intense peaks using Debye–Scherrer's equation, and the result is presented in Table 1. The result showed that the average crystal size of the biosynthesized ZnO NPs has decreased when the ratio of the plant extract increased from 9 : 1(26.7 nm) to 3 : 2 (22.6 nm) and to 1 : 1 (18.5 nm) ratio by volume. This is due to the fact that the greater amount of the plant extract used during the synthesis process results in effective capping and stabilizing the synthesized nanoparticles and hindered from aggregation. Table 1 also shows that the average crystal size

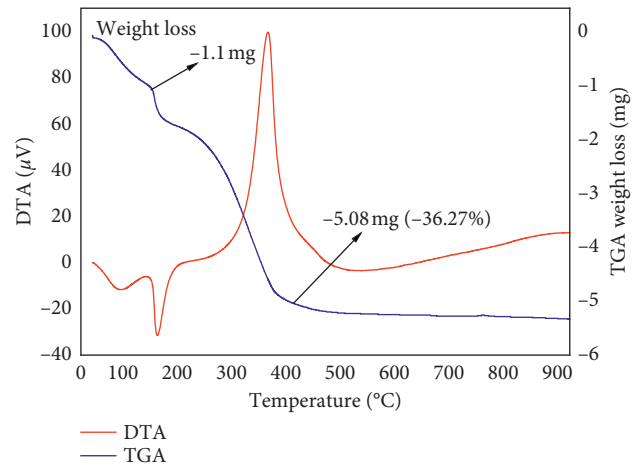

Figure 1: Thermal analysis of as-synthesized ZnO NPs using zinc acetate dihydrate and *Lippia adoensis* leaf extract in 9 : 1 ratio.

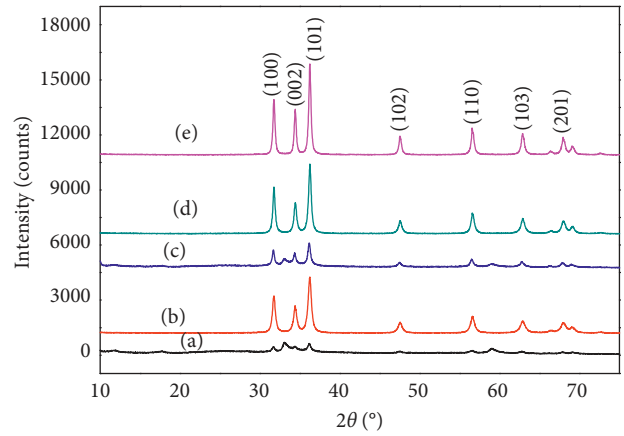

Figure 2: XRD patterns of ZnO NPs synthesized using zinc acetate dihydrate and *Lippia adoensis* leaf extract of different ratios by volume. (a) 1 : 1 (uncalcinated). (b) 1 : 1. (c) 3 : 2 (uncalcinated). (d) 3 : 2. (e) 9 : 1.

of uncalcinated ZnO NPs synthesized by using 1 : 1 and 3 : 2 ratios by volume of precursor salt and plant extract is less than their corresponding calcinated ZnO NPs. This may also be due to the high concentrations of biomolecules from plants that remain in the uncalcinated NPs that could highly stabilize the nanoparticles by capping and hinders further crystal growth.

3.3. Scanning Electron Microscopy-Energy Dispersive Spectroscopy (SEM-EDS) Analysis. The surface morphologies of biosynthesized ZnO nanoparticles were studied by using SEM, and the results are presented in Figure 3. Figure 3(a) shows the SEM image of as-synthesized ZnO NPs synthesized by using 1 : 1 ratio by volume of the reactants. The image shows spherical shapes in which the particles are also found to be inclined together due to the presence of more capping agent that stabilizes the nanoparticles. On the other hand, the morphology of calcinated ZnO nanoparticles synthesized from 1 : 1 and 3 : 2 ratios by volume of reactants

Table 1: FWHM values, average crystallite sizes calculated using Scherrer's formula, d-spacing ($d_{h\,k\,l}$), and Miller indices of calcinated and uncalcinated ZnO NPs synthesized using zinc acetate dihydrate and *Lippia adoensis* leaf extract at ratios by volume of 3 : 2, 1 : 1, and 9 : 1.

$h\,k\,l$	2θ (degree)	d-spacing ($d_{h\,k\,l}$)	3 : 2 ZnO NPs FWHM (degree)	3 : 2 UZnO NPs FWHM (degree)	1 : 1 ZnO NPs FWHM (degree)	1 : 1 UZnO NPs FWHM (degree)	9 : 1 ZnO NPs FWHM (degree)
1 0 0	31.7773	2.81369	0.35610	0.35010	0.44830	0.68000	0.30140
0 0 2	34.4411	2.60192	0.38560	0.41040	0.46960	1.18660	0.29280
1 0 1	36.2598	2.47548	0.39210	0.39870	0.48830	0.75380	0.30810
1 0 2	47.5471	1.91083	0.45350	0.45000	0.57290	0.65330	0.28000
1 1 0	56.6034	1.62471	0.43830	0.41840	0.55160	0.72000	0.34300
1 0 3	63.3832	1.46627	0.35500	0.45180	0.65800	0.80000	0.37210
2 0 0	66.4138	1.40671	0.46700	0.32400	0.66500	—	0.24580
1 1 2	67.9799	1.37788	0.55040	0.52670	0.70180	0.76000	0.27340
2 0 1	69.0795	1.35861	0.51600	0.45550	0.70660	0.78000	0.41430
Average crystallite size			22.6 nm	22.5 nm	18.5 nm	9 nm	26.7 nm

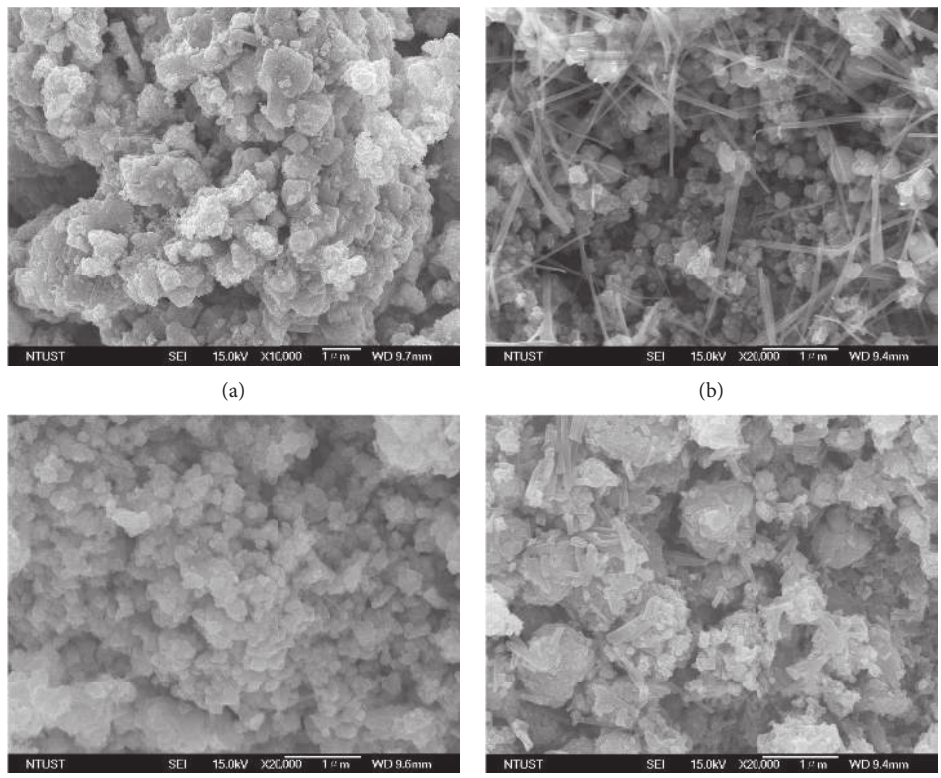

Figure 3: SEM images of (a) 1 : 1 UZnO, (b) 1 : 1 ZnO, (c) 3 : 2 ZnO, and (d) 9 : 1 ZnO NPs.

(Figures 3(b) and 3(c)) showed predominantly spherical in shape even though nanorod-shaped structures were also observed later. Furthermore, the SEM image of ZnO NPs synthesized from 9 : 1 reactant ratio by volume (Figure 3(d)), in which the amount of the salt precursor is much greater than the amount of plant extract, contains both nanorod- and flake-type shapes in aggregated form. This aggregation/agglomeration may be caused due to polarity and electrostatic attraction of ZnO nanoparticles [10].

To gain further insight into the features of the biosynthesized ZnO NPs, the analysis of the sample was performed using EDS techniques. The energy dispersive spectra of the samples obtained from the SEM-EDS analysis show that the sample prepared by using *Lippia adoensis* plant extract has pure ZnO phases. The EDS studies of Figure 4 present three peaks between 1 kV and 10 kV that are directly related to zinc in the tested material [21, 22]. The results indicate that the reaction product is composed of high-purity zinc nanoparticles, and the composition obtained from EDS analysis of the normalized spectrum was zinc (59.43%) and oxygen (40.57%). Additionally, the presence of highly pure ZnO is also confirmed by X-ray diffraction (Figure 2).

3.4. Transmission Electron Microscopy (TEM) Analysis. HRTEM with SAED analysis can be used to understand the crystalline characteristics and size of the synthesized

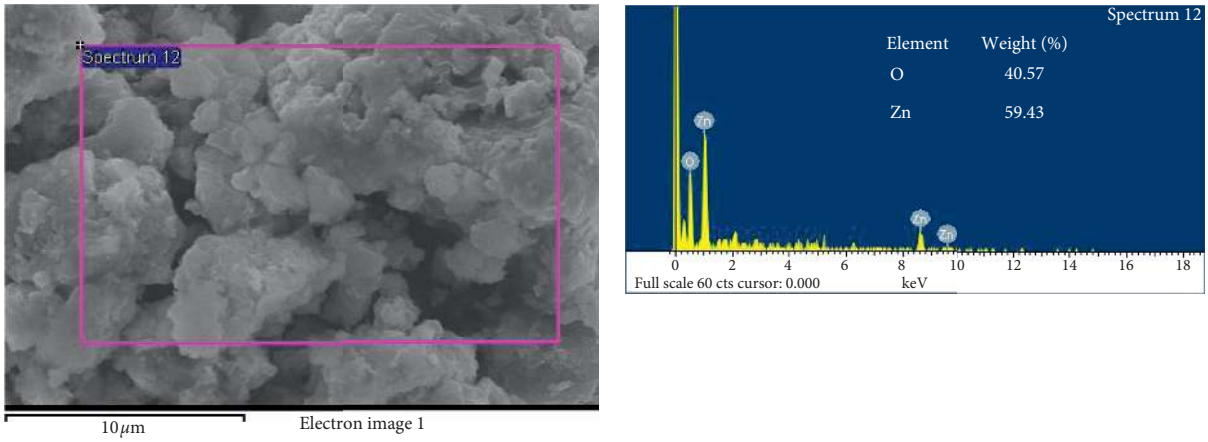

(a) (b)

Figure 4: SEM images of selected area for EDX spectra of (a) 1 : 1 UZnO EDX and (b) quantitative analysis.

nanoparticles [15]. The crystallography and morphology of biosynthesized ZnO nanoparticles were analyzed by TEM which is presented in Figure 5. The TEM image (Figure 5(a)) reveals that the biosynthesized ZnO NPs were agglomerated particles, spherical, and hexagonal wurtzite with an average particle size found to be 19.78 nm. This is well supported with the XRD values and has also shown to be spherical- and hexagonal-shaped particles. The crystalline nature of the synthesized ZnO nanoparticle is confirmed by the SAED pattern, which is represented in Figure 5(b). The SAED pattern indicates polycrystalline nature of the prepared ZnO nanoparticles [14]. Furthermore, from Figure 5(c), the 5 nm resolution studies of biosynthesized ZnO nanoparticles have shown 0.2446 nm "d" space, which further confirms the crystalline nature of nanoparticles.

3.5. Fourier Transform Infrared (FTIR) Analysis. The results of FTIR for uncalcinated and calcinated ZnO are shown in Figure 6. From Figure 6, different bands were observed at 3442 cm^{-1}, 2921 cm^{-1}, 2353 cm^{-1}, 1398 cm^{-1}, and 419 cm^{-1} and 3414 cm^{-1}, 2345 cm^{-1}, 1391 cm^{-1}, and 436 cm^{-1} for uncalcinated and calcinated ZnO nanoparticles, respectively. The FTIR spectra also exhibited a broad peak at around 3414 and 3442 cm^{-1} in a higher energy region due to O-H stretching of alcohols and phenols [36].

Absorption bands at 2345 and 2353 cm^{-1} are because of the presence of CO_2 molecules in the environment [37]. The peak at around 1591 cm^{-1} is due to the C-C stretching aromatic ring, and the strong intensity at 1401 cm^{-1} is due to α-CH_2 bending vibrations of aldehydes and ketones. The peak in the region between 400 and 600 cm^{-1} is assigned to Zn-O stretching vibration [38], confirming ZnO NPs are synthesized using *Lippia adoensis* extract as a reducing and capping agent.

3.6. Ultraviolet-Visible (UV-Vis) Spectral Analysis. Figure 7(a) shows UV-Vis absorption spectrum of zinc oxide nanoparticles. Strong absorption bands of the biosynthesized samples were observed from UV-visible spectra in the range of 360–363 nm which corresponds to the characteristic band of ZnO nanoparticles [39]. Absence of any other absorbance peak in the spectra confirms that the synthesized products are pure ZnO NPs. Furthermore, it is reported that the peak positions of UV-visible spectra are related with size of nanoparticles and blue shifted as the crystal size of the nanoparticles decreased [40]. The band-gap energies were calculated based on the numerical derivative of the optical absorption coefficient using Tauc's relationship between the optical absorption coefficient (α), the photon energy ($h\nu$), the constant (A), and the direct band-gap energy (E_g) (Figure 7(b)). Band-gap energy values were found to be 3.05, 3.11, and 3.21 eV for ZnO NPs synthesized from 9 : 1, 3 : 2, and 1 : 1 ratios, respectively, which is in close agreement with previously reported values [35]. The variation in E_g for the different ratios could be due to variation in average crystal size of the NPs.

3.7. Antibacterial Activity Analysis of ZnO Nanoparticles. The antibacterial activity of biosynthesized ZnO NPs was investigated against selected pathogens such as *Staphylococcus aureus*, *Enterococcus faecalis*, *Escherichia coli*, and *Klebsiella pneumonia* by using the disc diffusion method, and the result is shown in Table 2.

In general, as shown in Table 2, the biosynthesized ZnO NPs using *Lippia adoensis* leaf extract exhibited strong antibacterial activity against both Gram-positive (*S. aureus* and *E. faecalis)* and Gram-negative (*E. coli* and *K. pneumonia)* bacteria strains. Further, the result of antibacterial activity clearly indicated that the uncalcinated ZnO NPs in all concentration ranges showed a greater zone of inhibition against all bacterial strains compared to calcinated ZnO NPs. This may be due to the small crystal size of the uncalcinated nanoparticle and the synergetic antibacterial activity of the *Lippia adoensis* extract [31, 32]. Furthermore, the uncalcinated ZnO nanoparticles showed better antibacterial activity against Gram-positive than the Gram-negative bacterial strains. Previous research report also indicated bactericidal activity of ZnO nanoparticles was greater on Gram-positive than Gram-negative bacteria [41]. The reason for the difference

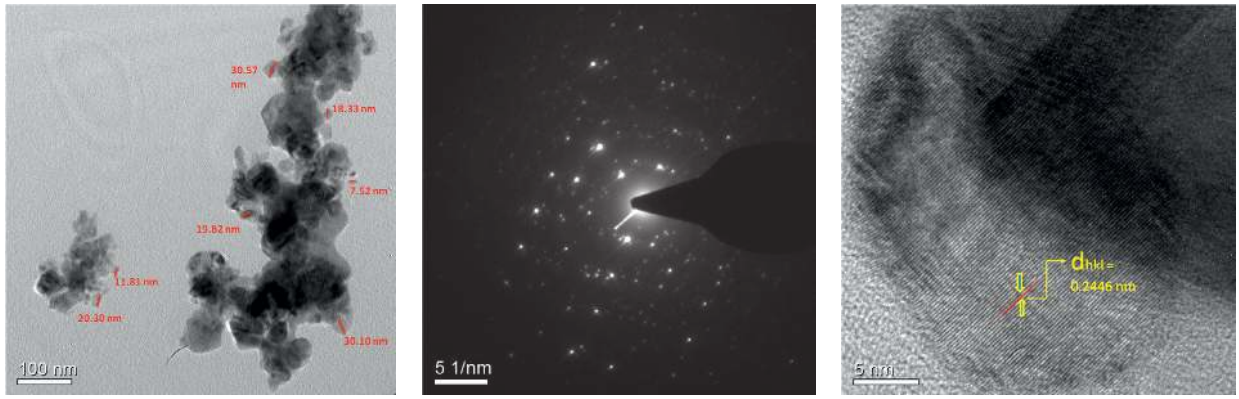

(a) (b) (c)

Figure 5: (a) TEM image, (b) SAED pattern, and (c) HRTEM image of biosynthesized ZnO NPs from zinc acetate dihydrate and leaf extract of *Lippia adoensis* in 1 : 1 ratio by volume.

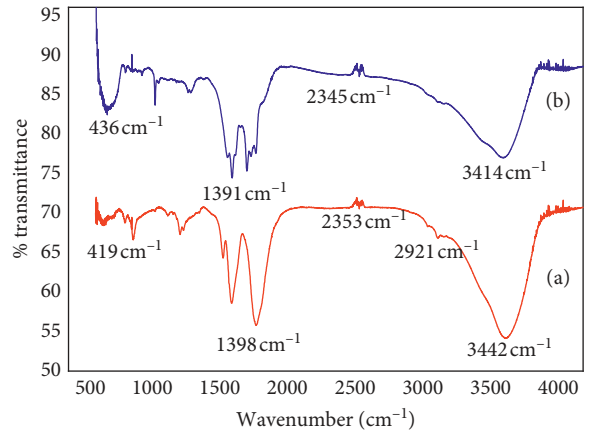

Figure 6: FTIR spectra of (a) uncalcinated and (b) calcinated ZnO NPs synthesized from zinc acetate dihydrate and *Lippia adoensis* leaf extract with 1 : 1 ratio by volume.

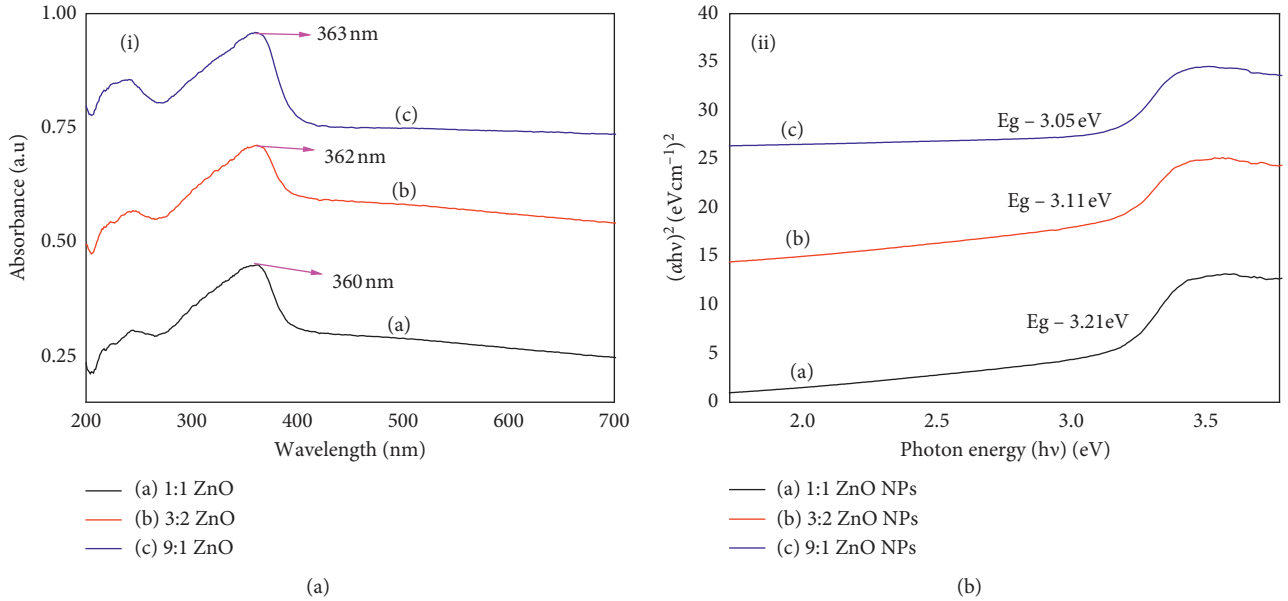

(a) (b)

Figure 7: (a) Absorption spectra and (b) Tauc plot of biosynthesized ZnO nanoparticles at different ratios by volume.

Table 2: Zone of inhibition (mm) of ZnO nanoparticles against Gram-positive and Gram-negative bacterial strains.

Samples	Conc. (mg/μL)	Zone of inhibition (mm) (diameter)			
		Gram-positive bacteria		Gram-negative bacteria	
		S. aureus	*E. faecalis*	*E. coli*	*K. pneumonia*
1 : 1 UZnO	1 : 2	14	10	9	12
	1 : 4	12	8	12	11
	1 : 8	12	8	9	10
1 : 1 ZnO	1 : 2	8	6	6	6
	1 : 4	8	6	8	6
	1 : 8	9	6	6	6
3 : 2 ZnO	1 : 2	8	6	6	6
	1 : 4	8	6	6	6
	1 : 8	8	6	6	8
9 : 1 ZnO	1 : 2	6	6	8	8
	1 : 4	7	6	6	6
	1 : 8	8	6	8	6
DMSO (N_C)	—	6	6	6	6
Carbenicillin (P_C)	—	—	—	6	8
Vancomycin (P_C)	—	14	10	—	—
ZnO NPS and antibiotic	—	16	14	13	10

in sensitivity between Gram-positive and Gram-negative bacteria might be attributed to the differences in morphological constitutions between these microorganisms. Gram-negative bacteria have an outer lipopolysaccharide membrane, and this makes the cell wall impermeable to antibacterial chemical substances. Gram-positive bacteria on the other hand are more susceptible having only an outer peptidoglycan layer which is not an effective permeability barrier. Therefore, the cell walls of Gram-negative bacteria are more complex in layout than the Gram-positive ones acting as a diffusion barrier and making them less susceptible to the antibacterial agents [34]. In addition, it was also reported that *Lippia adoensis* plant extract showed efficient antibacterial activity against Gram-positive bacterial strains [31, 32] that could also be accounted as another possible reason for the effectiveness of uncalcinated ZnO NPs against Gram-positive bacteria than Gram-negative bacteria as the plant extract may play synergetic effect.

For the ways of interactions of ZnO NPs with bacteria, scientists have suggested a few possible bactericidal mechanisms. Some proposed that smaller NPs have greater surface reactivity and easier cell penetration that released Zn^{2+}. The release of Zn^{2+} from ZnO NPs is one of the main propositions in antibacterial mechanisms which are known to inhibit several bacterial cell activities including active transport, bacteria metabolism, and enzyme activity leading to bacterial cell death due to the toxicity properties of Zn^{2+} [42]. The other proposed antibacterial activity is caused by the formation of reactive oxygen species (ROS) which leads to oxidative stress and subsequent cell damage or death. The formation of ROS is a common antibacterial activity adopted by ZnO NPs [43]. Another possible mechanism for the antimicrobial activity of ZnO NPs is through the attachment of NPs to the bacteria cell membrane via electrostatic forces. This interaction may distort the membrane plasma structure and damage the bacterial cell integrity, resulting in the leakage of intracellular contents and ends with cell death [44].

4. Conclusions

In this study, ZnO NPs were successfully synthesized from leaf extract of *Lippia adoensis* for the first time through a simple, cost-effective, ecofriendly, and green approach. This showed *Lippia adoensis* could potentially be used as an effective reducing and capping agent for biological synthesis of ZnO NPs. The biosynthesized ZnO NPs were characterized using techniques such as TGA, XRD, SEM-EDS, TEM, FTIR, and UV-Vis. From the TGA analysis, the biosynthesized ZnO NPs showed thermal stability above 400°C. The crystallinity of the biosynthesized ZnO NPs was proved from XRD analysis, and the analysis showed that all the diffraction peaks fit well with the hexagonal wurtzite structure. Furthermore, XRD analysis showed that the average crystal sizes of ZnO NPs synthesized from 3 : 2, 1 : 1, and 9 : 1 ratios by volume were found to be 22.6 nm, 18.5 nm, and 26.8 nm. SEM and TEM analysis showed that the morphology of the biosynthesized ZnO NPs was predominantly spherical in shape even though nanorod-shaped structures were also observed. Furthermore, the purity of the ZnO NPs was also confirmed from EDS analysis. The optical band-gap energies were determined from UV-Vis using the Tauc plot and found to be 3.11, 3.21, and 3.05 eV for ZnO NPs synthesized from 3 : 2, 1 : 1, and 9 : 1 ratios by volume, respectively. Further, the biosynthesised ZnO nanoparticles using *Lippia adensis* leaf extract have proved themselves to be an effective antibacterial agent against both Gram-positive (*S. aureus* and *E. feacalis)* and Gram-negative (*E. coli* and *K. pneumonia)* bacteria suggesting strong and promising action of green-synthesized ZnO nanoparticles against biological systems.

Data Availability

The data used to support the findings of this study are available from the corresponding author upon request.

Disclosure

The funder, Adama Science and Technology University, has not been involved in editing, approval, or decision to publish this manuscript. The funder has no issue of conflicts of interest with authors concerning submission and publication of this research work.

Conflicts of Interest

The authors declare that they have no conflicts of interest.

Acknowledgments

The authors would like to acknowledge Adama Science and Technology University for financial support, Applied Chemistry Department and Material Science and Engineering Department at Adama Science and Technology University for allowing them to use XRD for characterization of the samples, and also Taiwan National University, Department of Material Science and Engineering Laboratory, for allowing them to use UV-visible spectroscopy, EDX, and SEM. This research work was supported by Adama Science and Technology University through its 12th cycle research grant.

References

[1] M. C. David, M. Ebrahim, V. C. Ada et al., "Green nanotechnology-based zinc oxide (ZnO) nanomaterials for biomedical applications: a review," *Journal of Physics: Materials*, vol. 3, no. 3, Article ID 034005, 2020.

[2] V. N. Kalpana and R. V. Devi, "A review on green synthesis, biomedical applications and toxicity studies of ZnO NPs," *Bioinorganic Chemistry and Applications*, vol. 2018, 12 pages, Article ID 3569758, 2018.

[3] H. A. Bilal, S. Muzamil, S. H. Syed et al., "Green bio-assisted synthesis, characterization and biological evaluation of biocompatible ZnO NPs synthesized from different tissues of milk thistle (Silybum marianum)," *Nanomaterials*, vol. 9, no. 8, p. 1171, 2019.

[4] A. Muthuvinothini and S. Stella, "Green synthesis of metal oxide nanoparticles and their catalytic activity for the reduction of aldehydes," *Process Biochemistry*, vol. 77, pp. 48–56, 2019.

[5] G. Yanli, X. Dan, R. Dan, Z. Kaifang, and W. Xiyu, "Green synthesis of zinc oxide nanoparticles using Citrus sinensis peel extract and application to strawberry preservation: a comparison study," *Food Science and Food Safety*, vol. 126, Article ID 109297, 2020.

[6] M. Nilavukkarasi, S. Vijayakumar, and S. Prathipkumar, "Capparis zeylanica mediated bio-synthesized ZnO nanoparticles as antimicrobial, photocatalytic and anti-cancer applications," *Materials Science for Energy Technologies*, vol. 3, pp. 335–343, 2020.

[7] A. Waseem and K. Divya, "Green synthesis, characterization and anti-microbial activities of ZnO nanoparticles using Euphorbia hirta leaf extract," *Journal of King Saud UniversityScience*, vol. 32, no. 4, pp. 2358–2364, 2020.

[8] X. Zheng, W. Yuhui, S. Ling, C. Arunachalam, A. A. Sulaiman, and F. Liwei, "Anticarcinogenic effect of zinc oxide nanoparticles synthesized from Rhizoma paridis saponins on Molt-4 leukemia cells," *Journal of King Saud University-Science,* vol. 32, no. 3, pp. 1865–1871, 2020.

[9] E. T. Bekele, B. A. Gonfa, O. A. Zelekew, H.H. Belay, and F. K. Sabir, "Synthesis of titanium oxide nanoparticles using root extract of kniphofia foliosa as a template, characterization, and its application on drug resistance bacteria," *Journal of Nanomaterials*, vol. 2020, p. 10, Article ID 2817037, 2020.

[10] S. Vijayakumar, B. Vaseeharan, B. Malaikozhundan, and M. Shobiya, "Laurus nobilis leaf extract mediated green synthesis of ZnO nanoparticles: characterization and biomedical applications," *Biomedicine & Pharmacotherapy*, vol. 84, pp. 1213–1222, 2016.

[11] M. D. Mauricio, S. Guerra-Ojeda, P. Marchio et al., "Nanoparticles in medicine: a focus on vascular oxidative stress," *Oxidative Medicine and Cellular Longevity*, vol. 2018, p. 20, Article ID 6231482, 2018.

[12] M. Seyyed, H. M. Tabrizi, E. Behrouz, and J. Vahid, "Biosynthesis of pure zinc oxide nanoparticles using Quince seed mucilage for photocatalytic dye degradation," *Journal of Alloys and Compounds*, vol. 821, Article ID 153519, 2020.

[13] N. I. Rasli, H. Basri, and Z. Harun, "Zinc oxide from aloe vera extract: two-level factorial screening of biosynthesis parameters," *Heliyon*, vol. 6, no. 1, Article ID e03156, 2020.

[14] S. Vijayakumar, P. Arulmozhi, N. Kumar, B. Sakthivel, S. Prathip Kumar, and P. K. Praseetha, "*Acalypha fruticosa* L. leaf extract mediated synthesis of ZnO nanoparticles: characterization and antimicrobial activities," *Materials Today: Proceedings*, vol. 23, pp. 73–80, 2020.

[15] A. Muthuvel, M. Jothibas, and C. Manoharan, "Effect of chemically synthesis compared to biosynthesized ZnO-NPs using Solanum nigrum leaf extract and their photocatalytic, antibacterial and *in vitro* antioxidant activity," *Journal of Environmental Chemical Engineering*, vol. 8, no. 2, Article ID 103705, 2020.

[16] B. Niranjan, S. Saha, M. Chakraborty et al., "Green synthesis of zinc oxide nanoparticles using Hibiscus subdariffa leaf extract: effect of temperature on synthesis, anti-bacterial activity and anti-diabetic activity," *RSC Advances*, vol. 5, no. 7, pp. 4993–5003, 2015.

[17] H. M. Yusof, R. Mohamad, U. H. Zaidan, and N. A. A. Rahman, "Microbial synthesis of zinc oxide nanoparticles and their potential application as an antimicrobial agent and a feed supplement in animal industry: a review," *Journal of Animal Science and Biotechnology*, vol. 10, no. 1, p. 57, 2019.

[18] D. T. Handago, A. Z. Enyew, and A. G. Bedasa, "Effects of Azadirachta indica leaf extract, capping agents, on the synthesis of pure and Cu doped ZnO-nanoparticles: a green approach and microbial activity," *Open Chemistry*, vol. 17, no. 4, pp. 246–465, 2019.

[19] M. J. Haque, M. M. Bellah, M. R. Hassan, and S. Rahman, "Synthesis of ZnO nanoparticles by two different methods & comparison of their structural, antibacterial, photocatalytic and optical properties," *Nano Express*, vol. 1, no. 1, Article ID 010007, 2020.

[20] J. Santhoshkumar, S. V. Kumar, S. Rajeshkumar, and G. Adaikalaraj, "Synthesis of zinc oxide nanoparticles using plant leaf extract against urinary tract infection pathogen," *Resource-Efficient Technologies*, vol. 3, no. 6, pp. 459–1651, 2017.

[21] A. Chaudhary, N. Kumar, R. Kumar, and R. Kumar, "Antimicrobial activity of zinc oxide nanoparticles synthesized from *Aloe vera* peel extract," *SN Applied Sciences*, vol. 1, no. 1, p. 136, 2019.

[22] K. Elumalai, S. Velmurugan, K. Ravi et al., "Bio-approach: plant mediated synthesis of ZnO nanoparticles and their catalytic reduction of methylene blue and antimicrobial activity," *Advanced Powder Technology*, vol. 26, no. 3, pp. 1639–1651, 2015.

[23] D. Renata and D. Jolanta, "Biosynthesis and antibacterial activity of ZnO nanoparticles using Trifolium pratense flower Extract," *Saudi Journal of Biological Sciences*, vol. 23, no. 4, pp. 517–523, 2016.

[24] G. Sharmila, C. Muthukumaran, K. S. Sandiya et al., "Biosynthesis, characterization, and antibacterial activity of zinc oxide nanoparticles derived from *Bauhinia tomentosa* leaf extract," *Journal of Nanostructure in Chemistry*, vol. 8, no. 3, pp. 293–299, 2018.

[25] A. A. Mohammad, M. Mahadevamurthy, P. Daruka et al., "*Cinnamomum verum* bark extract mediated green synthesis of ZnO nanoparticles and their antibacterial potentiality," *Biomolecules*, vol. 10, pp. 134–336, 2020.

[26] I. Shagufta, S. Amna, A. A. Aftab et al., "Green tea leaves mediated ZnO nanoparticles and its antimicrobial activity," *Cogent Chemistry*, vol. 4, no. 1, Article ID 1469207, 2018.

[27] D. Suresh, R. M. Shobharani, P. C. Nethravathi, M. A. P. Kumar, H. Nagabhushana, and S. Sharma, "Artocarpus gomezianus aided green synthesis of ZnO nanoparticles: luminescence, photocatalytic and antioxidant properties," *Spectrochimica Acta Part A: Molecular and Biomolecular Spectroscopy*, vol. 141, pp. 128–164, 2015.

[28] M. S. Shekhawat, C. P. Ravindran, and M. Manokari, "Biogenic production of zinc oxide nanoparticles from aqueous extracts of *Duranta erecta* L," *World Scientific News*, vol. 28, p. 30, 2016.

[29] K. Elumalai, S. Velmurugan, S. Ravi, V. Kathiravan, and S. Ashokkumar, "Green synthesis of Zinc oxide nanoparticles using Moringa oleifera leaf extract and evaluation of its antimicrobial activity," *Spectrochimica Acta Part A: Molecular and Biomolecular Spectroscopy*, vol. 143, pp. 158–164, 2015.

[30] O. O. Solabomi, A. Yasmine, Z. Muchen et al., "Green synthesis of zinc oxide nanoparticles using different plant extracts and their antibacterial activity against Xanthomonas oryzae pv. Oryzae," *Artificial Cells, Nanomedicine, and Biotechnology*, vol. 47, no. 1, pp. 341–352, 2019.

[31] A. B. Gemechu, G. D. Abdella, and D. Engda, "Antimicrobial activity of *Lippia adoensis* var. koseret against human pathogenic bacteria and fungi," *American Journal of Clinical and Experimental Medicine*, vol. 3, no. 3, p. 118, 2015.

[32] W. Yared, A. Tesfalem, and A. Solomon, "Evaluation of antibacterial activity and phytochemical constituents of leaf extract of Lippia adoensis," *Asia Pacific Journal of Energy and Environment*, vol. 1, no. 1, 2014.

[33] D. R. Sharmila and R. Gayathri, "Green synthesis of zinc oxide nanoparticles by using Hibiscus rosa-sinensi," *International Journal of Current Engineering and Technology*, vol. 4, no. 1, p. 1137, 2014.

[34] A. M. Getie, A. Belay, A. R. Chandra Reddy, and Z. Belay, "Synthesis and Characterizations of Zinc Oxide Nanoparticles for Antibacterial Applications," *Journal of Nanomedicine & Nanotechnology*, vol. 8, no. 9, pp. 2157–2524, 2017.

[35] T. Xaba, P. P. Mongwai, M. Lesaoana, P. Khatri, and L. Mahadi, "Decomposition of bis(N-benzyl-salicydenaminato)zinc(II) complex for the synthesis of ZnO nanoparticles to fabricate ZnO chitosan nanocomposite for the removal of iron(II) Ions from wastewater," *Journal of Chemistry*, vol. 2019, 9 pages,, Article ID 1907083, 2019.

[36] M. Awwad, B. Albiss, L. Ahmad, A. J. Nathanael, S. I. Hong, and V. Au, "Green synthesis, characterization and optical properties of zinc oxide nanosheets using Olea euro pea leaf extract," *Advanced Materials Letters*, vol. 5, pp. 250–258, 2014.

[37] P. Jamdagni, K. Poonam, and J. S. Rana, "Green synthesis of zinc oxide nanoparticles using flower extract of Nyctanthes arbor-tristis and their antifungal activity," *Journal of King Saudi University-Science*, vol. 30, no. 2, pp. 168–175, 2018.

[38] R. Yuvakkumar, J. Suresh, B. Saravanakumar, A. J. Nathanaeld, S. I. Honga, and Rajendran, "Rambutan peels promoted biomimetic synthesis of bioinspired zinc oxide nanochains for biomedical applications," *Spectrochimica Acta Part A: Molecular and Biomolecular Spectroscopy*, vol. 137, pp. 250–258, 2015.

[39] A. A. Salahuddin, W. F. Kemary, E. M. Ibrahim et al., "Synthesis and characterization of ZnO nanoparticles via precipitation method: effect of annealing temperature on particle size," *Journal of Nanoscience and Nanotechnology*, vol. 5, no. 2, pp. 82–218, 2015.

[40] P. M. Pranjali, M. P. Pooja, J. D. Maruti et al., "Synthesis and characterization of zinc oxide nanoparticles by using polyol chemistry for their antimicrobial and antibiofilm activity," *Biochemistry and Biophysics Reports*, vol. 17, pp. 71–151, 2019.

[41] A. Tayel, W. El-Tras, S. Moussa, A. El-Baz, and H. Mahrous, "Antibacterial action of zinc oxide nanoparticles against food borne pathogens," *Journal of Food Safety*, vol. 31, no. 2, pp. 211–218, 2011.

[42] S. Soren, S. Kumar, S. Mishra et al., "Evaluation of antibacterial and antioxidant potential of the zinc oxide nanoparticles synthesized by aqueous and polyol method," *Microbial Pathogenesis*, vol. 90, pp. 78–84, 2018.

[43] H. Agarwal, S. Menon, S. V. Kumar, and S. Rajeshkumar, "Mechanistic study on antibacterial action of zinc oxide nanoparticles synthesized using green route," *Chemico-Biological Interactions*, vol. 286, pp. 60–70, 2018.

[44] C. Jayaseelan, A. A. Rahuman, A. V. Kirthi, S. Marimuthu, T. Santhoshkumar, and A. Bagavan, "Novel microbial route to synthesize ZnO nanoparticles using Aeromonas hydrophila and their activity against pathogenic bacteria and fungi," *Spectrochimica Acta Part A: Molecular and Biomolecular Spectroscopy*, vol. 90, pp. 78–84, 2012.